THE JOURNAL OF BIOLOGICAL CHEMISTRY VOL. 287, NO. 7, pp. 4925–4935, February 10, 2012

Hypercholesterolemia Induces Up-regulation of K_{ACh} Cardiac Currents via a Mechanism Independent of Phosphatidylinositol 4,5-Bisphosphate and G$\beta\gamma$*[S]

Received for publication, September 21, 2011, and in revised form, December 7, 2011 Published, JBC Papers in Press, December 15, 2011, DOI 10.1074/jbc.M111.306134

Wu Deng[‡1], **Anna N. Bukiya**[§], **Aldo A. Rodríguez-Menchaca**[‡], **Zhe Zhang**[‡], **Clive M. Baumgarten**[‡], **Diomedes E. Logothetis**[‡], **Irena Levitan**[¶], **and Avia Rosenhouse-Dantsker**[¶2]

From the [¶]*Department of Medicine, Pulmonary Section, University of Illinois at Chicago, Chicago, Illinois 60612, the* [‡]*Department of Physiology and Biophysics, Virginia Commonwealth University School of Medicine, Richmond, Virginia 23298, and the* [§]*Department of Pharmacology, The University of Tennessee Health Science Center, Memphis, Tennessee 38163*

Background: K_{ACh} channels play a key role in controlling the heart rate.
Results: K_{ACh} currents are enhanced by cholesterol enrichment and high cholesterol diet.
Conclusion: Cholesterol plays a critical role in modulating $I_{K,ACh}$ in atrial cardiomyocytes.
Significance: The increase in $I_{K,ACh}$ following cholesterol enrichment is likely to play a critical role in hypercholesterolemia-induced dysfunction of the heart.

Hypercholesterolemia is a well-known risk factor for cardiovascular disease. In the heart, activation of K_{ACh} mediates the vagal (parasympathetic) negative chronotropic effect on heart rate. Yet, the effect of cholesterol on K_{ACh} is unknown. Here we show that cholesterol plays a critical role in modulating K_{ACh} currents ($I_{K,ACh}$) in atrial cardiomyocytes. Specifically, cholesterol enrichment of rabbit atrial cardiomyocytes led to enhanced channel activity while cholesterol depletion suppressed $I_{K,ACh}$. Moreover, a high-cholesterol diet resulted in up to 3-fold increase in $I_{K,ACh}$ in rodents. In accordance, elevated currents were observed in *Xenopus* oocytes expressing the Kir3.1/Kir3.4 heteromer that underlies $I_{K,ACh}$. Furthermore, our data suggest that cholesterol affects $I_{K,ACh}$ via a mechanism which is independent of both $PI(4,5)P_2$ and G$\beta\gamma$. Interestingly, the effect of cholesterol on $I_{K,ACh}$ is opposite to its effect on I_{K1} in atrial myocytes. The latter are suppressed by cholesterol enrichment and by high-cholesterol diet, and facilitated following cholesterol depletion. These findings establish that cholesterol plays a critical role in modulating $I_{K,ACh}$ in atrial cardiomyocytes via a mechanism independent of the channel's major modulators.

Control of the heart rate is a complex process that integrates the function of multiple proteins, such as G protein-coupled receptors and ion channels. Among them, G protein-regulated inwardly rectifying K^+ (GIRK[3] or Kir3) channels play a major role (1–4). Kir3 channels are important in regulating membrane excitability in cardiac, neuronal, and endocrine cells (5). Loss of Kir3 channel activity leads to cardiac abnormalities (6), neuronal hyperexcitability, and seizures in the brain (7, 8), hyperactivity and reduced anxiety (9). In the heart, the atrial K_{ACh} channels are heterotetrameric proteins that consist of two pore-forming subunits, Kir3.1 (GIRK1) and Kir3.4 (GIRK4) (10). Activation of K_{ACh} by acetylcholine (ACh) (6, 11, 12) via the muscarinic M2 receptor and pertussis toxin-sensitive G proteins mediates the vagal negative chronotropic effect (1–4). Thus, activation of K_{ACh} channels can terminate paroxysmal supraventricular tachycardia (PSVT), *i.e.* a rapid cardiac rhythm (13). On the other hand, vagal stimulation predisposes to atrial fibrillation (AF) (14), which can lead to thromboembolism and stroke (15, 16). Thus, while Kir3.4 knock-out mice exhibit a mild tachycardia and blunted heart rate regulation by M2 receptors (17), Kir3.4 knock-out mice are also resistant to AF caused by vagal stimulation without any change in atrioventricular node function or ventricular arrhythmias (14).

We recently reported cholesterol sensitivity of representative homomeric Kir channels using the *Xenopus* oocyte heterologous expression system (18). Kir3.4*, the highly active Kir3.4 pore mutant S143T that has similar characteristics to those of the Kir3.1/Kir3.4 complex (19), was stimulated by cholesterol. Cholesterol is one of the major lipid components of the plasma membrane in mammalian cells. While cholesterol is essential for cell function and growth, its excess is associated with multiple pathological conditions (20–22) including development of cardiovascular disease (23–25). Thus, the present study was designed to examine the impact of cholesterol on cardiac K_{ACh} currents ($I_{K,ACh}$).

EXPERIMENTAL PROCEDURES

Expression of Recombinant Channels in Xenopus Oocytes—Point mutations on the background of control Kir3.4_S143T (Kir3.4*) (19) were generated using the QuickChange site-di-

* This work was supported, in whole or in part, by National Institutes of Health Grants HL-073965, HL-083298 (to I. L.), and HL-059949 (to D. E. L.) and Scientist Development Grant 11SDG5190025 from the American Heart Association (to A. R.-D.).
[S] This article contains supplemental Figs. S1 and S2.
[1] Supported by National Institutes of Health Training Grant 5T32HL094290.
[2] To whom correspondence should be addressed: Department of Medicine, Pulmonary Section, University of Illinois at Chicago, Chicago, IL 60612. Fax: 312-996-4665; E-mail: dantsker@uic.edu.
[3] The abbreviations used are: GIRK, G protein-regulated inwardly rectifying K^+; MβCD, methyl-β-cyclodextrin; TEVC, two-electrode voltage clamp; GTPγS, guanosine 5′-3-*O*-(thio)triphosphate; ACh, acetylcholine; $PI(4,5)P_2$, phosphatidylinositol 4,5-bisphosphate; AF, atrial fibrillation.

rected mutagenesis kit (Stratagene). cRNAs were transcribed *in vitro* using the MessageMachine kit (Ambion). Oocytes were isolated and microinjected as previously described (26). Expression of channel proteins in *Xenopus* oocytes was accomplished by injection of the desired amount of cRNA, 2 ng per oocyte for Kir3.4* or Kir3.4*D223N, and for coexpression of Kir3.1 with Kir3.4, 1 ng per oocyte per channel. All oocytes were maintained at 17 °C. Two-electrode voltage clamp recordings were performed 2 days after injection.

Two-electrode Voltage-clamp Recording and Analysis (Xenopus Oocytes)—Whole-cell currents were measured by conventional two-microelectrode voltage clamp with a GeneClamp 500 amplifier (Axon Instruments), as previously reported (26). A high-potassium (HK) solution was used to superfuse oocytes (in mM: 96 KCl, 1 NaCl, 1 $MgCl_2$, 5 HEPES KOH buffer, pH 7.4). Basal currents represent the difference of inward currents obtained (at −80 mV) in the presence and absence of 3 mM $BaCl_2$ in high-potassium solution. Each experiment was performed on a minimum of 3–5 oocytes from the same batch, and a minimum of two batches of oocytes were tested for each normalized recording shown. Recordings from different batches of oocytes were normalized by the mean of whole-cell basal currents from untreated oocytes. Statistics (mean ± S.E.) for each construct were calculated from all of the normalized data from different batches of oocytes. Statistical analysis of the data was performed using a two-tailed Student's t test with $p < 0.05$ taken to be significant. The fitting of the curves for the time courses was performed using Origin software (Originlab).

Macropatch Recording (Xenopus Oocytes)—Currents were recorded from the inside-out patch configuration using an EPC9 amplifier (HEKA) and the Pulse fit program (HEKA). The bath and pipette solutions of ND96K+EGTA were composed of 96 mM KCl, 1 mM $MgCl_2$, 5 mM EGTA, and 10 mM HEPES, pH 7.4. Currents were recorded at a holding membrane potential of −80 mV.

Ci-VSP Rundown Experiments in Xenopus Oocytes and Their Analysis—Ci-VSP (28) has a voltage sensor coupled to a phosphoinositide phosphatase, leading to dephosphorylation of $PI(4,5)P_2$. The phosphatase activity is activated by membrane depolarization (28). The advantage of this method of depleting $PI(4,5)P_2$ is that it allows to examine the effect of dephosphorylation of $PI(4,5)P_2$ on whole-cell currents using two-electrode voltage clamp rather than by inside-out recording from macropatches. As with other methods that remove $PI(4,5)P_2$, activation of Ci-VSP results in current rundown, and rundown is slower and less complete with stronger interaction of the channel with $PI(4,5)P_2$. Activation of Ci-VSP is achieved by cycling between −80 mV and +80 mV. The rundown curves for each experiment (oocyte) were fitted to an exponential decay function of a second order: $\text{Inhibition} = \text{Inhibition}_{(t=\infty)} + A_1\exp(-t/\tau_1) + A_2\exp(-t/\tau_2)$. The limiting value, $\text{Inhibition}_{(t=\infty)}$, is the maximal inhibition that would be obtained at infinity. The average of the values obtained in all the experiments is given in the summary figure.

Cholesterol Enrichment of Xenopus Oocytes—A 1:1:1 (w/w/w) mixture containing cholesterol, porcine brain L-α-phosphatidylethanolamine (PE) and 1-palmitoyl-2-oleoyl-sn-glycero-3-phospho-L-serine (PS) (Avanti Polar Lipids, Birmingham, AL) was evaporated to dryness under a stream of nitrogen. The resultant pellet was suspended in a buffered solution consisting of 150 mM KCl and 10 mM Tris/HEPES at pH 7.4, and sonicated at 80 kHz (Laboratory Supplies, Hicksville, NY). *Xenopus* oocytes were treated with cholesterol for 1 h.

Cholesterol Enrichment and Depletion of Atrial Cardiomyocytes—As previously described (25), cardiomyocytes were depleted of cholesterol by exposure to the cholesterol acceptor methyl-β-cyclodextrin (MβCD). Alternatively, cells are enriched with cholesterol by treatment with MβCD saturated with cholesterol, a well-known cholesterol donor. Depletion was carried out with freshly prepared 5 mM MβCD in a modified Kraft-Brühe solution (pH 7.2) for 30 min or 1 h. For enrichment, an MβCD-cholesterol solution was prepared as described previously (29). In brief, a small volume of cholesterol solvated in chloroform was added to a glass tube, the solvent was evaporated, and then 5 mM MβCD in a modified Kraft-Brühe solution (pH 7.2) was added to the dried cholesterol. This preparation was sonicated and incubated overnight in a rotating bath at 37 °C. The cells were incubated with the MβCD-cholesterol solution for 1 h. During enrichment and depletion, myocytes were maintained in a humidified CO_2 incubator at 37 °C. After treatment, cells were washed three times with serum-free medium and returned to the incubator.

Rat High Cholesterol Diet—A group of 25-day-old male Sprague-Dawley rats was placed on a high-cholesterol diet (2% cholesterol in standard rodent food) (Harland-Teklad). Another group of the same age was fed an isocaloric, cholesterol-free diet from the same supplier. Rats were sacrificed as atrial tissue donors after 20–24 weeks on control or high cholesterol diet.

Atrial Myocyte Isolation—Atrial myocytes were freshly isolated from adult New Zealand White rabbits (2.8–3.1 kg) of either gender or from male rats by a Pronase-collagenase enzymatic dissociation method. Hearts were excised, immediately tied via the aorta to a Langendorff column, and retrogradely perfused for 5 min with Tyrode solutions that were oxygenated and maintained at 37 °C, followed by 5 min with a Ca^{2+}-free Tyrode solution. The heart was then perfused with enzyme solution for ~20 min. Atria were excised, minced, and placed in fresh enzyme solution. The tissues were bubbled with an O_2/CO_2 (95%:5%) gas mixture and gently shaken for two 15-min cycles in a 37 °C shaker bath. At the end of each cycle the supernatant was collected and replaced with fresh enzyme solution. Supernatants were filtered through 200 μm nylon, and isolated cells were pelleted by gentle centrifugation. Isolated myocytes were stored in a modified Kraft-Brühe solution (pH 7.2) before using. Rod-shaped quiescent cells with clear striations and no membrane blebs or other morphological irregularities were studied within 10 h of isolation. Tyrode solution for myocyte isolation contained (mM): 130 NaCl, 5 KCl, 1.8 mM $CaCl_2$, 0.4 KH_2PO_4, 3 $MgCl_2$, 5 HEPES, 15 taurine, 5 creatine, 10 glucose, pH 7.25 (adjusted with NaOH). For Ca^{2+}-free Tyrode solution, $CaCl_2$ was replaced with 0.1 mM Na_2EGTA. For making enzyme solution, the Ca^{2+}-free Tyrode solution was supplemented with 0.45 mg/ml collagenase (Cls 4; Worthington Biochemical) and 0.015 mg/ml Pronase (Type XIV; Sigma-Aldrich). The modified Kraft-Brühe myocyte storage

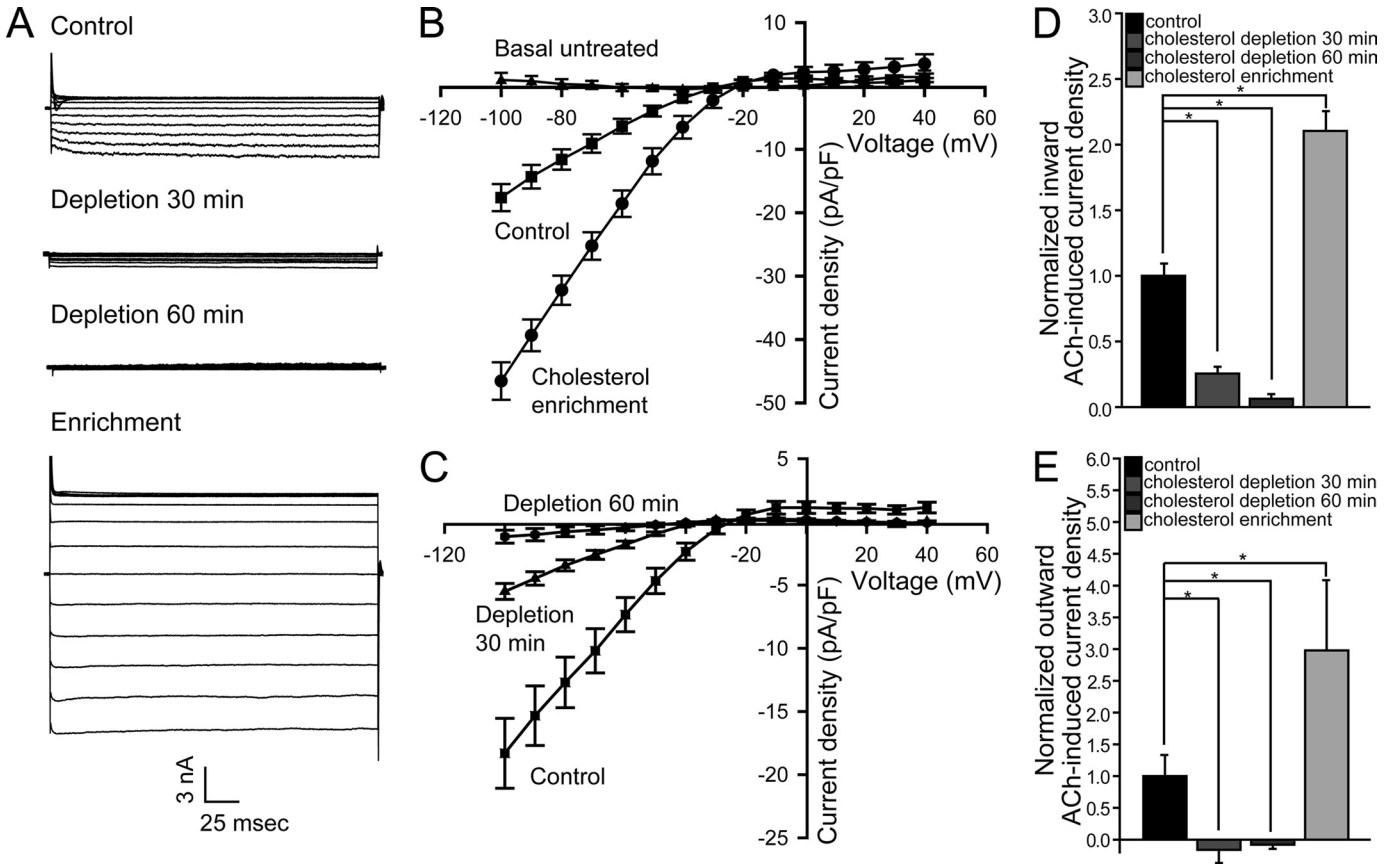

FIGURE 1. **ACh-induced currents in atrial cardiomyocytes are enhanced by cholesterol.** Tertiapin-sensitive currents (*A*) and I-V relationships (*B* and *C*) of ACh-induced current densities for control and cholesterol-treated myocytes. Also shown in *B* are tertiapin-insensitive basal current densities. Summary data: (*D*) inward ACh-induced current densities at −80mV; (*E*) outward ACh-induced current densities at +40mV. Significant difference is indicated by an *asterisk* (*, $p < 0.05$); ($n = 6–13$). Recordings were done using cells from 2–4 rabbits per treatment.

solution contained (mM): 120 K-glutamate, 10 KCl, 10 KH_2PO_4, 0.5 K_2EGTA, 10 taurine, 1.8 $MgSO_4$, 10 HEPES, 20 glucose, 10 mannitol, pH 7.2 (adjust with KOH).

Whole Cell Patch Clamp and Electrophysiological Recordings (Atrial Myocytes)—Pipettes were pulled using a P-97 micropipette puller (Sutter Instrument) and then fire polished. The final pipette tip diameter was 2–3 μm, and the corresponding pipette resistance in bath solution was 2–4 MΩ. Junction potentials were corrected, and a 3 M KCl-agar bridge served as the ground electrode. Freshly isolated atrial myocytes were dispersed over a glass-bottomed cell chamber (~0.3 ml) and extracellular solution was superfused at a rate of 2–3 ml/min. Typical seal resistances were 5–10 GΩ. Myocytes were dialyzed for at least 5 min before data were collected. After obtaining the whole-cell configuration, successive 250 ms long steps were applied from −50 mV or −80 mV to test potentials between −100 and +40 mV in +10 mV increments, and current-voltage (I-V) relationships were plotted from quasi steady-state currents. Currents were recorded with an Axoclamp 200B and Digidata 1322A under pClamp 9 (MDS Analytical Technology) and digitized (5 kHz) after low-pass filtering (Bessel, 2 kHz). The high-K/low-Cl extracellular solution contained (mM): $NaMeSO_3$ 90, $KMeSO_3$ 30, KCl 20, $CaCl_2$ 0.5, $MgCl_2$ 1.0, HEPES 10, pH 7.4. Pipette solution contained (mM): K-aspartate 110, KCl 20, NaCl 10, $MgCl_2$ 1.0, Na_2-ATP 2.0, EGTA 2.0 Na_2-GTP 0.01 HEPES 10, pH 7.4. ACh activation was obtained using 10 μM ACh (Sigma), and 100 nM tertiapin-Q (30) (Tocris) was used to block the channels. Tertiapin-sensitive currents were obtained by subtracting the currents recorded after perfusion of tertiapin from the currents of the control and cholesterol-treated ACh-induced currents, and from the basal currents, respectively. To examine the effect of GTPγS, 100 μM GTPγS were added to the pipette solution, and the myocytes were dialyzed for at least 10 min before data were collected. After basal currents were obtained, the cells were superfused with ACh containing solution followed by a solution containing both ACh and tertiapin-Q. Currents recorded were normalized to cell size by dividing the amplitude of the current (pA) by the capacitance of the cell (pF) to obtain the current density. Statistics (mean ± S.E.) for each construct were calculated from all of the normalized data from different batches of myocytes. Statistical analysis of the data were performed using a two-tailed Student's *t* test or a one-way ANOVA, and comparisons to the control group were made by the Holm-Sidak method with $p < 0.05$ taken to be significant.

RESULTS

ACh-induced Currents in Atrial Cardiomyocytes Are Up-regulated by Cholesterol—To investigate the role of cholesterol in modulating cardiac K_{ACh} currents ($I_{K,ACh}$), we first examined the effect of both cholesterol enrichment and depletion on $I_{K,ACh}$ in atrial cardiomyocytes. As Fig. 1, *A* and *B*, shows, cho-

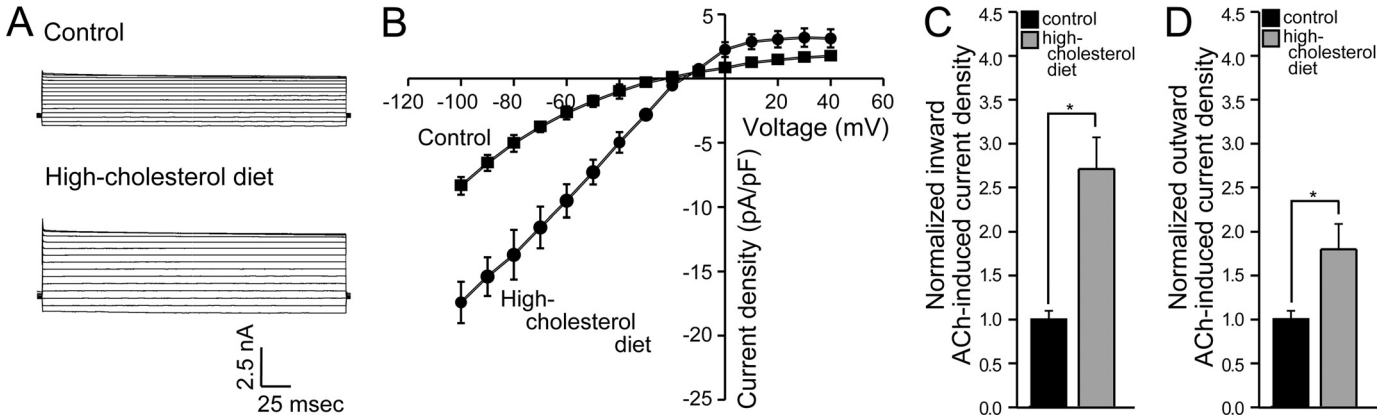

FIGURE 2. **ACh-induced currents in atrial cardiomyocytes are enhanced in hypercholesterolemic animals.** Tertiapin-sensitive currents (*A*) and I-V relationships (*B*) of ACh-induced current densities for atrial myocytes from control and hypercholesterolemic rats. Summary data: (*C*) inward ACh-induced current densities at −80 mV; (*D*) outward ACh-induced current densities at +40 mV. Significant difference is indicated by an *asterisk* (*, $p < 0.05$). Recordings were done using cells from 2 rats per condition.

lesterol enrichment by exposing myocytes for 1 h to methyl-β-cyclodextrin (MβCD) saturated with cholesterol, a well-known cholesterol donor (29), resulted in an ~2-fold increase in K_{ACh} currents that were sensitive to the selective $I_{K,ACh}$-blocker tertiapin (30). Conversely, cholesterol depletion following a 30-min exposure to untreated MβCD, which acts as a cholesterol acceptor (29), decreased cardiomyocyte $I_{K,ACh}$ (Fig. 1, *A* and *C*). Further exposure to MβCD for one hour suppressed $I_{K,ACh}$ currents almost completely. Summary data in Fig. 1, *D* and *E* show that cholesterol enrichment and depletion modulated both inward and outward currents in a similar manner. Thus, while the effect was more visible for the larger inward currents, the physiologically relevant smaller outward currents were also significantly affected by cholesterol.

High Cholesterol Diet Enhances K_{ACh} Currents in Atrial Myocytes—Following our finding that acute cholesterol enrichment enhances K_{ACh} currents in atrial cardiomyocytes, we next evaluated the tertiapin-sensitive K_{ACh} currents in atrial myocytes from rats subject to a hypercholesterolemic diet. As can be seen in Fig. 2, *A–D*, rats that were on high cholesterol diet for 20–24 weeks exhibited up to 2–3-fold increase in both inward and outward K_{ACh} currents.

Basal Currents in Atrial Cardiomyocytes Are Down-regulated by Cholesterol—In addition to Kir3.1/Kir3.4 channels that underlie $I_{K,ACh}$, atrial cardiomyocytes also express inwardly rectifying potassium channels, which are members of the Kir2 family and underlie I_{K1} (31). We previously showed that cholesterol enrichment suppresses whereas cholesterol depletion enhances Kir2 currents in endothelial cells and heterologously expressed channels in CHO cells or *Xenopus* oocytes (18, 32–34). Interestingly, the inwardly rectifying non-$I_{K,ACh}$-induced basal currents in atrial cardiomyocytes, which are not sensitive to tertiapin, were regulated in an opposite fashion compared with $I_{K,ACh}$-induced currents (Fig. 3). Specifically, cholesterol enrichment resulted in approximately a 30% decrease in basal currents, whereas cholesterol depletion resulted in about a 70% increase. Furthermore, similarly to our observations in cholesterol-enriched myocytes, high-cholesterol diet resulted in approximately a 60% decrease in basal currents as can be seen in Fig. 3, *D–F*. Thus, the effect of cholesterol on basal currents was similar to its effect on members of the Kir2 subfamily.

Cholesterol Enrichment of Xenopus Oocytes Leads to Increased Kir3.1/Kir3.4 Currents—To gain mechanistic insight into the effect of cholesterol on K_{ACh} currents, we turned to the *Xenopus* oocyte heterologous expression system. This system is well suited for expression of proteins following cRNA injection, since it contains accumulated stores of enzymes, organelles and proteins that can be recruited for heterologous proteins (35), allowing basal activation of Kir3 currents (36). As Fig. 4 shows, the heterotetrameric Kir3.1/Kir3.4 channel that underlies $I_{K,ACh}$ rendered an ionic current that was facilitated by cholesterol enrichment, albeit to a lesser extent than Kir3.4*. In contrast, the homomer Kir3.1* was suppressed by elevated levels of cholesterol. Because Kir3.4* exhibits enhanced basal currents following cholesterol enrichment similarly to Kir3.1/Kir3.4 in atrial myocytes, we used it as a model system, and confirmed the results obtained using Kir3.1/Kir3.4.

Cholesterol Has a Subtle Effect on Kir3 Channel-PI(4,5)P_2 Interactions—The activity of Kir3 channels depends on PI(4,5)P_2, and requires the presence of an additional gating molecule, such as the βγ subunits of G proteins that may enhance channel-PI(4,5)P_2 interactions (27, 37). Thus, to gain mechanistic insight into the effect of cholesterol on $I_{K,ACh}$, we first examined whether cholesterol acts through PI(4,5)P_2 using *Xenopus* oocytes. It was previously shown that channel run-down following macropatch excision is associated with PI(4,5)P_2 dephosphorylation (27). Therefore, when the channel binds more strongly to PI(4,5)P_2, the rundown is slower. We thus examined the effect of cholesterol enrichment on current run-down. As depicted in supplemental Fig. S1*A*, the ionic current run-down of cholesterol-enriched oocytes was slightly slower than that of Kir3.4* in absence of cholesterol (control).

To further explore whether PI(4,5)P_2 could account for the cholesterol effect, we utilized Ci-VSP, a protein whose voltage sensor is coupled to a phosphoinositide phosphatase that dephosphorylates PI(4,5)P_2 to PI(4)P following membrane depolarization (28). The advantage of this method is that it allows us to examine the effect of dephosphorylation of PI(4,5)P_2 on whole-cell currents from intact cells using two-

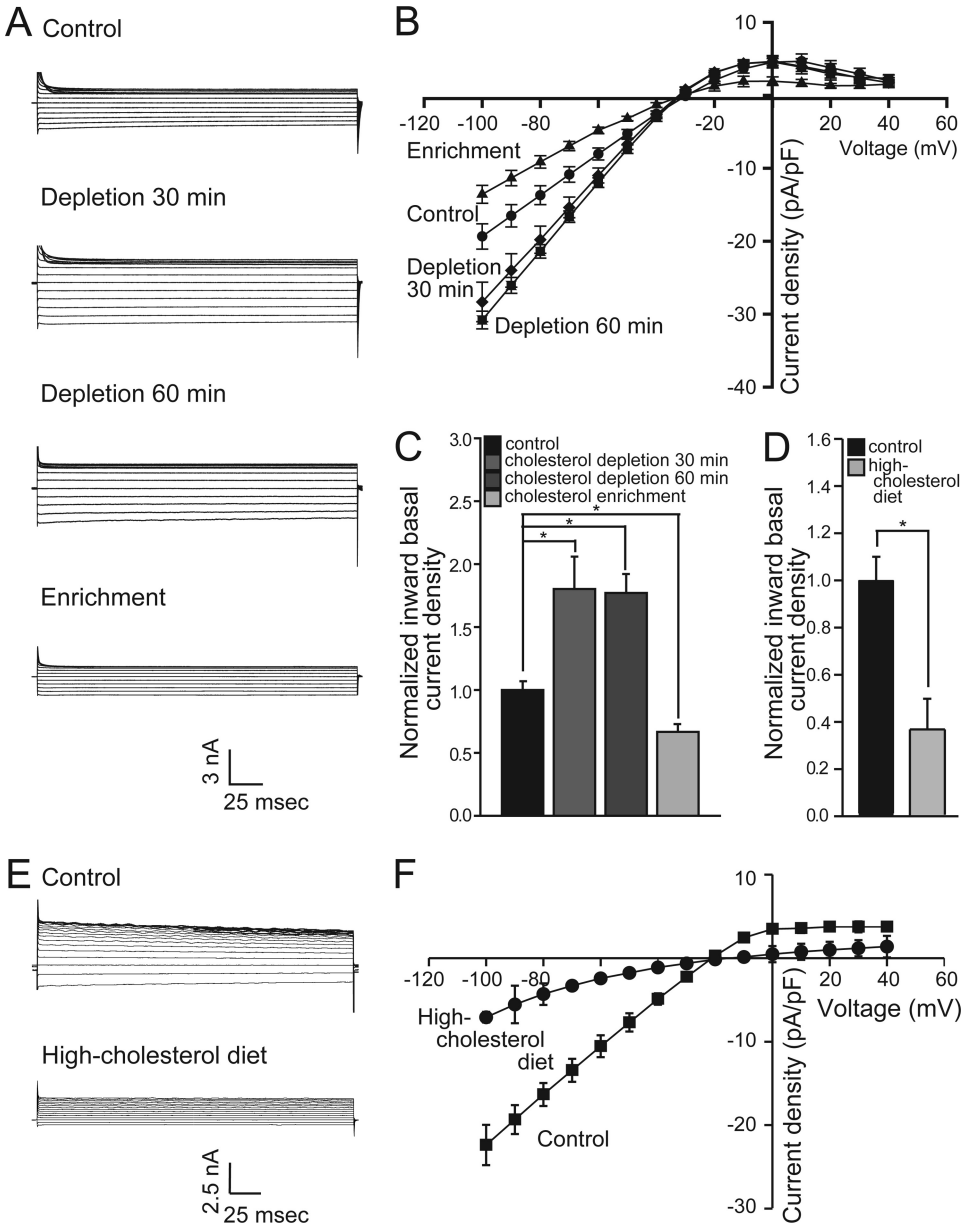

FIGURE 3. **Basal currents in atrial cardiomyocytes are suppressed by cholesterol.** (*A*) currents and (*B*) I-V relationships of basal current densities for control and cholesterol-treated myocytes. *C*, summary data for inward basal current densities at −80 mV ($n = 6–13$). Recordings were done using cells from 2–4 rabbits per treatment. *D*, summary data at −80 mV, (*E*) representative traces and (*F*) I-V relationships of basal current densities for atrial myocytes from control and hypercholesterolemic rats. Significant difference is indicated by an *asterisk* (*, $p < 0.05$). Recordings were done using cells from 2 rats per condition.

electrode voltage clamp (TEVC) rather than by inside-out recording from membrane macropatches. As with other methods that deplete $PI(4,5)P_2$, activation of Ci-VSP results in current run-down, and run-down is slower and less complete when the interaction of the channel with $PI(4,5)P_2$ is stronger. Before examining the effect of cholesterol enrichment on Kir3.4* current rundown, we tested the effect of coexpressing Ci-VSP with Kir3.4* on the consequences of cholesterol enrichment. As can be seen in supplemental Fig. S1*B* when compared with Fig. 4*B*, mere coexpression of Ci-VSP with Kir3.4* did not alter the effect of cholesterol enrichment on Kir3.4* currents. We then proceeded to activate Ci-VSP by cycling between −80 mV and +80 mV to deplete $PI(4,5)P_2$. As can be seen in Fig. 5, *A* and *B*, activation of Ci-VSP by depolarization caused a rapid decrease of Kir3.4* whole-cell currents to 12% of their initial value exhibited prior to Ci-VSP activation. In cholesterol-enriched oocytes, however, the current decreased to 18% of its initial value. Similarly, a small difference was also observed between control and cholesterol-enriched oocytes in the inhibition of Kir3.1/Kir3.4 currents following Ci-VSP activation (Fig. 5, *C* and *D*).

Could this small difference reflect that $PI(4,5)P_2$ interaction with the channel was slightly strengthened by cholesterol enrichment? The strength of channel-$PI(4,5)P_2$ interactions has been found to correlate strongly with current amplitude (38). We proceeded to examine the effect of Ci-VSP on the D223N mutant of Kir3.4*, whose interaction with $PI(4,5)P_2$ is significantly stronger than that of Kir3.4* (39), and whose

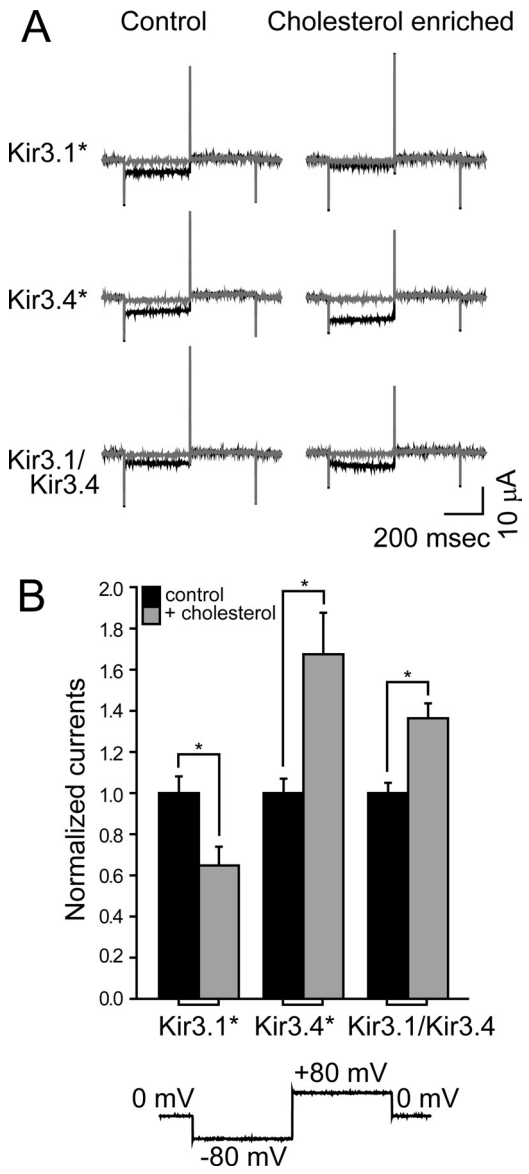

FIGURE 4. **Cholesterol enrichment of *Xenopus* oocytes leads to increased K_{ACh} currents.** Whole-cell basal currents recorded in oocytes at −80 mV showing the effect of cholesterol enrichment on Kir3.1*, Kir3.4*, and Kir3.1/Kir3.4. *A*, representative traces. *B*, summary data ($n = 20–34$). The currents are normalized relative to untreated oocytes expressing the same channel. The waveform is shown at the *bottom* of the figure. The *black traces* were obtained following application of high-potassium (*HK*) solution, and the *gray curves* were obtained when $BaCl_2$ was added to the HK solution (see under "Experimental Procedures"). Significant difference is indicated by an *asterisk* (*, $p < 0.05$).

whole-cell currents are comparable with the currents of Kir3.4* following cholesterol enrichment (Fig. 5*E*). As expected, D223N currents decreased only to 56% of their initial value following the activation of Ci-VSP (Fig. 5, *A* and *B*). Furthermore, since D223N not only exhibited stronger channel-$PI(4,5)P_2$ interactions than Kir3.4* but could also be activated by $PI(4,5)P_2$ alone (39), we examined the effect of this mutation on cholesterol sensitivity. As can be seen in Fig. 5*F*, cholesterol failed to stimulate D223N currents. This result is similar to our earlier observation regarding the effect on cholesterol sensitivity of mutating position 229, which is located in the cytosolic CD loop across from D223 (see Fig. 5*G*). Specifically, the I229L mutation also abrogates the cholesterol sensitivity of Kir3.4* (18). Notably, this mutation also strengthens channel-$PI(4,5)P_2$ interactions (27). In summary, cholesterol stimulated Kir3.4* currents to levels comparable to Kir3.4*D223N but did not affect the currents of this mutant. Whereas dephosphorylation of $PI(4,5)P_2$ by Ci-VSP greatly reduced Kir3.4* or cholesterol-stimulated Kir3.4* currents, it had a significantly smaller effect on Kir3.4*D223N currents. These results suggest that the mechanism by which cholesterol affects Kir3 currents cannot be accounted for by a strengthening of channel-$PI(4,5)P_2$ interactions, at least in a manner similar to that achieved with the D223N mutation.

Cholesterol Affects Kir3 Channels via a Gβγ-independent Mechanism—Next, we proceeded to examine the relationship of cholesterol sensitivity to gating mechanisms other than $PI(4,5)P_2$, such as that by the βγ subunits of G proteins. As can be seen in Fig. 6, *A* and *B*, the sensitivity of both Kir3.4* and Kir3.1/Kir3.4 to cholesterol was abrogated by coexpression of $G\beta_1\gamma_2$, suggesting that a Gβγ-related mechanism could play a direct role in cholesterol modulation of Kir3 channels.

Notably, however, since both cholesterol enrichment and increased levels of Gβγ enhance Kir3 currents (see supplemental Fig. S2, *A* and *B*), it is possible that the cholesterol sensitivity of Kir3 channels was abrogated following coexpression of $G\beta_1\gamma_2$ due to saturation of the currents by the βγ subunits of the G protein. Thus, to further investigate this possibility, we examined the effect of GTPγS on cholesterol sensitivity of $I_{K,ACh}$ in atrial myocytes following cholesterol depletion. All heterotrimeric G proteins employ a signaling strategy in which the metastable GTP-bound state of the Gα subunit is used as a molecular clock (40, 41). When GTP is hydrolyzed to GDP, Gα is inactivated, and its affinity for free Gβγ is increased. The potential contributions of G protein turnover to the kinetics of G protein-mediated signaling can be eliminated with the hydrolysis-resistant GTP analog, GTPγS. Binding of GTPγS to Gα persistently activates G proteins, constraining both Gα and Gβγ to their active states, reducing the signaling pathway to diffusion-limited interactions between Gβγ and the channel (40, 41). As can be seen in Fig. 6, *C* and *D*, in the presence of GTPγS in atrial myocytes, cholesterol depletion did not affect K_{ACh} currents. As expected and in contrast, GTPγS did not affect cholesterol modulation of Kir2 basal currents whose activation does not depend on Gβγ (Fig. 6*E*).

A simple explanation of our findings is that cholesterol may modulate Kir3 channels via a Gβγ-related mechanism. It is also possible, however, that in the presence of elevated levels of Gβγ, stabilization of the channel in its open state becomes dominant. Thus, utilizing the versatility of the *Xenopus* oocyte heterologous expression system, we carried out the following additional experiments: (1) examination of the effect of coexpression of Kir3.4* and of Kir3.1/Kir3.4 with the pH domain of the β adrenergic receptor kinase, βARK-PH, a Gβγ scavenger (42–44) (supplemental Fig. S2, *C* and *D*), on cholesterol sensitivity; (2) examination of the effect of the E339Q mutation of Kir3.4*, which impairs agonist-induced sensitivity and decreases binding to $G\beta_1\gamma_2$ (43) (supplemental Fig. S2*E*). As can be seen in Fig. 7, *A–C*, in all cases, the sensitivity of the

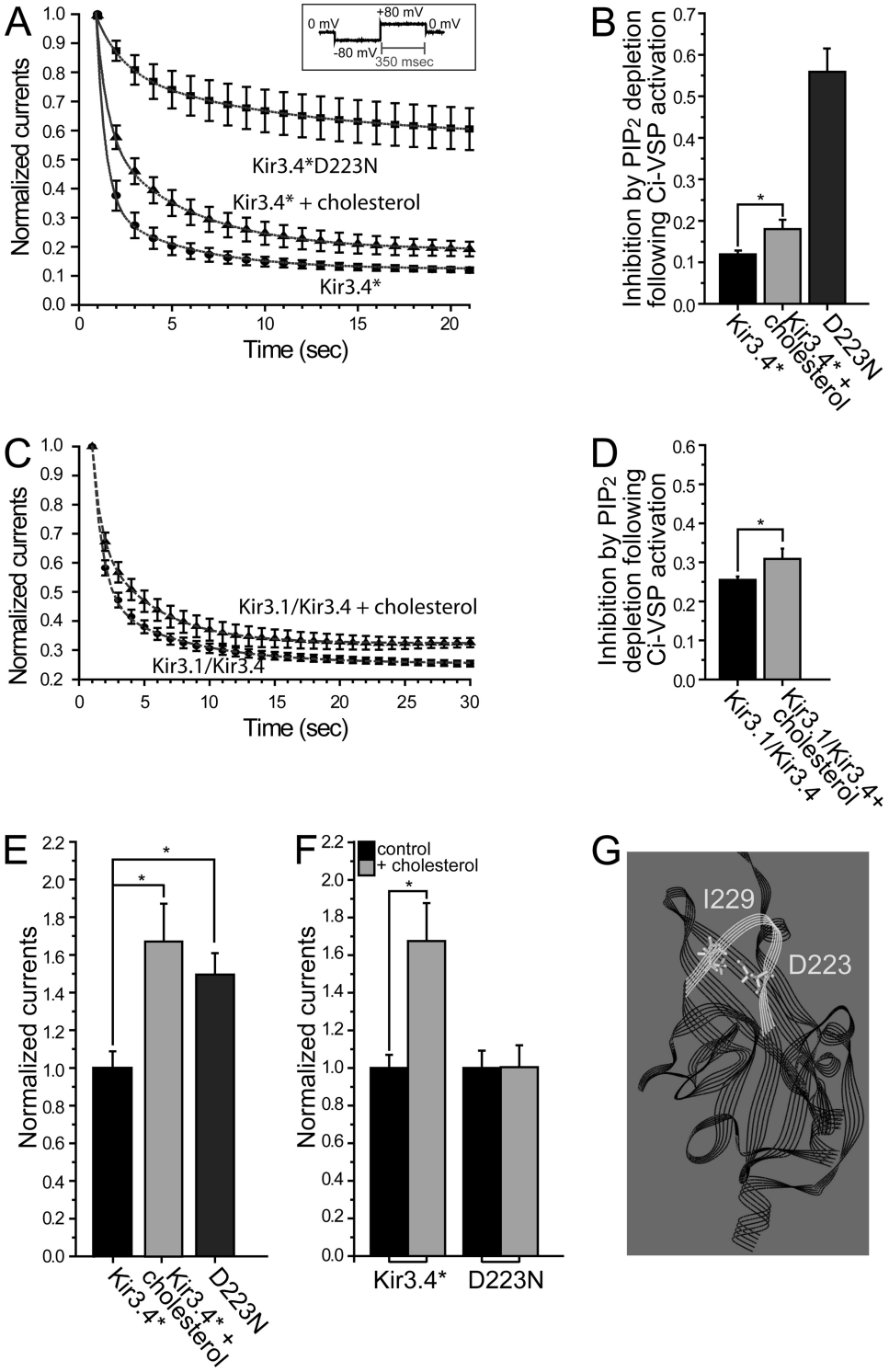

FIGURE 5. **Cholesterol has a subtle effect on Kir3 channel-PI(4,5)P_2 interactions.** *A–D*, current run-down of (*A*) Kir3.4* and (*C*) Kir3.1/Kir3.4 at −80 mV for control and cholesterol-enriched oocytes following PI(4,5)P_2 dephosphorylation upon Ci-VSP activation at +80 mV. The *inset* in *A* shows the protocol used. Also shown in *A* is current rundown of Kir3.4*D223N ($n = 6$ each). *B* and *D*, summary data based on *A* and *C* showing the extent of current inhibition following PI(4,5)P_2 dephosphorylation. *E*, whole-cell currents recorded in oocytes at −80 mV for Kir3.4* and Kir3.4*D223N. All currents are normalized relative to Kir3.4*. As a comparison, the effect of cholesterol enrichment of oocytes expressing Kir3.4* is also shown. *F*, whole-cell currents recorded at −80 mV for control (untreated) and cholesterol-enriched oocytes expressing Kir3.4* and Kir3.4*D223N. For each pair, the currents are normalized relative to untreated control oocytes expressing the same channel ($n = 12–34$). *G*, model of the cytosolic domain of Kir3.4 based on the crystallographic structure of the chimera between the cytosolic domain of Kir3.1 and the transmembrane domain of KirBac1.3 (PDB ID 2qks) showing D223 and I229 in the CD loop of the channel. Significant difference is indicated by an *asterisk* (*, $p < 0.05$).

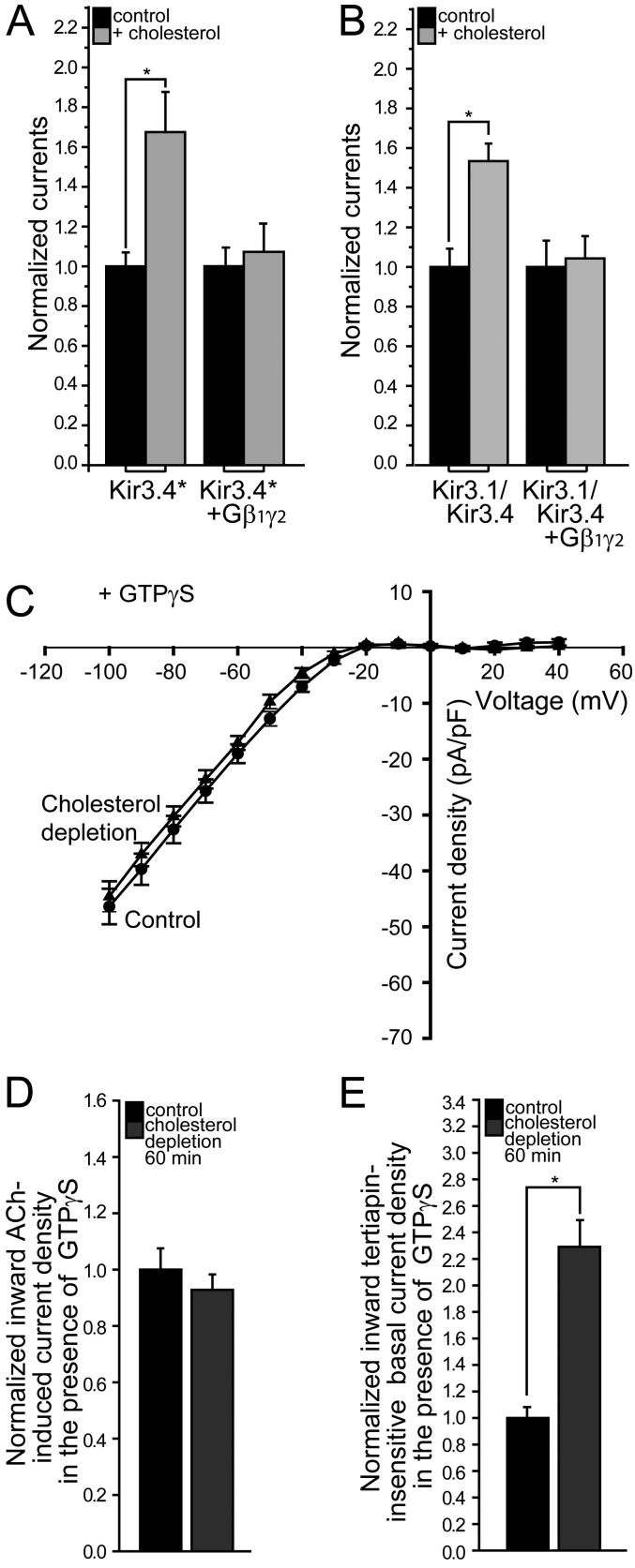

FIGURE 6. **Elevated levels of Gβγ dominate cholesterol modulation of Kir3 channels.** Whole-cell currents were recorded at −80mV for control and cholesterol-enriched oocytes expressing (*A*) Kir3.4* (n = 15–34) and (*B*) Kir3.1/Kir3.4 (n = 11–12), alone and coexpressed with $G\beta_1\gamma_2$. For each pair, the currents are normalized relative to control untreated oocytes expressing the same constructs. *C*, tertiapin-sensitive I-V relationships of $I_{K,ACh}$ in the presence of GTPγS for control and cholesterol-depleted atrial myocytes (n = 8–9). *D*, summary data for $I_{K,ACh}$ at −80 mV in the presence of GTPγS. *E*, summary data for tertiapin-insensitive whole-cell inward current densities at −80 mV in the presence of GTPγS. Significant difference is indicated by an *asterisk* (*, $p < 0.05$); (n = 8–9).

channel to cholesterol was not affected compared with the control channel, suggesting that Gβγ is not necessary for cholesterol modulation of Kir3 channels, and that cholesterol acts independently of Gβγ (Fig. 7*D*).

DISCUSSION

The major finding of this study is that cholesterol has a substantial facilitating effect on K_{ACh} channels function in atrial cardiomyocytes. This was observed both following cholesterol cell enrichment (Fig. 1) and in myocytes from rats subject to high-cholesterol diet (Fig. 2). Consistent with these observations, cholesterol depletion resulted in decreased $I_{K,ACh}$ (Fig. 1).

Interestingly, in myocytes that express both Kir2 and Kir3 channels, cholesterol has an opposite effect on basal and ACh-induced currents. Thus, whereas under basal stimulation conditions cholesterol enrichment inhibits Kir2 channels, upon stimulation, the dominant effect becomes facilitation of $I_{K,ACh}$. Furthermore, a facilitatory effect of cholesterol on K_{ACh} channels is unique because the majority of Kir channels are suppressed by cholesterol (18). Differential effects of cholesterol on different types of Kir channels expressed in the same cells may play a major role in fine-tuning the impact of hypercholesterolemia on heart function.

Moreover, our data demonstrate that even within the same Kir subfamily, the impact of cholesterol may vary. Whereas cholesterol enhances Kir3.4* and Kir3.1/Kir3.4, it suppresses Kir3.1* channels. This surprising observation may underlie the reduced sensitivity of the heteromer Kir3.1/Kir3.4 to cholesterol compared with Kir3.4*.

Our data suggest that cholesterol-induced facilitation of K_{ACh} currents should be attributed to a mechanism independent of $PI(4,5)P_2$. Specifically, Fig. 5, *A–D*, argues that the effect of cholesterol on channel gating is not predominantly by stabilizing the channel-$PI(4,5)P_2$ activated state. Moreover, Fig. 5*F* argues that the channel-$PI(4,5)P_2$-stabilized activated state occludes any further cholesterol effect. Thus, since Fig. 5, *A–D* suggest that $PI(4,5)P_2$ stabilization of the cholesterol-activated state is a small component of the effect, cholesterol may be acting by a distinct mechanism to stabilize the open state of the channel. Once the open state is stabilized by another mechanism (*e.g.* strengthening of channel-$PI(4,5)P_2$ interactions by Gβγ), cholesterol does not produce a further effect as evident in Fig. 6, *A–D*. In accord, when the open state is not stabilized by another mechanism (*e.g.* following the removal of Gβγ), cholesterol plays a major role in channel gating as Fig. 7, *A–C* demonstrate. This interpretation is consistent with our recent work (45) showing that the cholesterol sensitivity of Kir2.1 depends on a belt of residues, which are correlated with the major cytosolic gate of the channel, the G-loop (46). Thus, the $PI(4,5)P_2$ and the cholesterol- active states are likely to reflect a common open conducting channel state of Kir3.1/Kir3.4.

In contrast and similarly to our previous studies of the effect of cholesterol on Kir2 channels in other cells (18, 32, 33), cho-

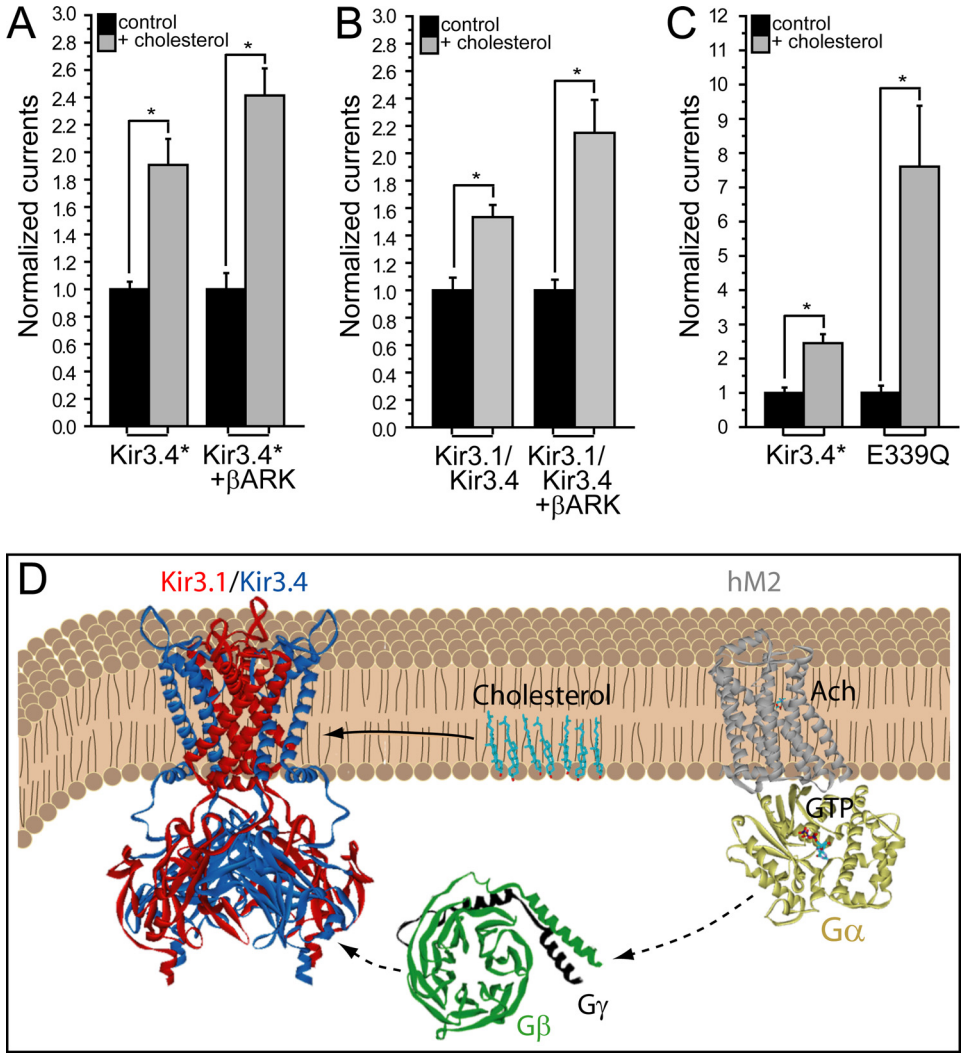

FIGURE 7. **Cholesterol modulation of Kir3 channel is independent of Gβγ.** Whole-cell currents were recorded at −80 mV for control and cholesterol-enriched oocytes expressing (*A*) Kir3.4* (n = 12–20) and (*B*) Kir3.1/Kir3.4 (n = 10–12), alone and coexpressed with βARK-PH. *C*, whole-cell currents recorded at −80 mV for control and cholesterol-enriched oocytes expressing Kir3.4* and Kir3.4*E339Q (n = 10–12). For each pair in *A–C*, the currents are normalized relative to control untreated oocytes expressing the same construct. *D*, schematic model illustrating that cholesterol modulates K_{ACh} channels independent of the βγ subunits of the G protein.

lesterol increase inhibits I_{K1} in atrial myocytes, an effect that has been previously attributed to direct Kir2-cholesterol interactions (34) and to stabilization of the channel in its closed state (33). Furthermore and similarly to the effect of high-cholesterol diet on endothelial cells isolated from hypercholesterolemic animals (47), also in atrial myocytes high-cholesterol diet resulted in significantly lower Kir2 currents compared with cells isolated from control animals. Thus, cholesterol may regulate different Kir channels by opposite mechanisms. Accordingly, whereas cholesterol stabilizes the closed state of Kir2 channels, it stabilizes the open state of Kir3.1/Kir3.4.

Since hypercholesterolemia is a risk factor for cardiovascular disease, the increase in $I_{K,ACh}$ following cholesterol enrichment and in hypercholesterolemic animals is likely to play a key role in the function of the heart. It was previously shown that chronic atrial fibrillation patients exhibit agonist-independent constitutive K_{ACh} activity that contributes to the enhanced basal inward rectifier current (48). Corresponding constitutively active $I_{K,ACh}$-like currents are up-regulated by canine atrial tachypacing (49, 50). In addition, selective blocking of $I_{K,ACh}$ by tertiapin results in action potential prolongation and suppression of inducible atrial-fibrillation (50). Thus, cholesterol-induced up-regulation of K_{ACh} activity may also contribute significantly to the development of atrial fibrillation. Moreover, statins, which are cholesterol lowering drugs, have been suggested as potential treatment for preventing AF (51). Yet, the diverse mechanisms by which statins could reduce AF onset are uncertain (52). Thus, our findings may explain the association of statins to decreased risk of AF, and may lead to a novel therapeutic approach to prevent and reverse AF.

Acknowledgments—We thank Heikki Vaananen and Sophia Gruszecki (VCU) for oocyte preparation, Alex Dopico for facilitating studies on hypercholesterolemic animals and critical reading of the manuscript, and Maria Asuncion-Chin (UTHSC) for technical assistance in experiments on rat myocytes.

REFERENCES

1. Breitwieser, G. E., and Szabo, G. (1985) Uncoupling of cardiac muscarinic and β-adrenergic receptors from ion channels by a guanine nucleotide analogue. *Nature* **317,** 538–540
2. Kurachi, Y., Nakajima, T., and Sugimoto, T. (1986) Acetylcholine activation of K^+ channels in cell-free membrane of atrial cells. *Am. J. Physiol.* **251,** H681–H684
3. Pfaffinger, P. J., Martin, J. M., Hunter, D. D., Nathanson, N. M., and Hille, B. (1985) GTP-binding proteins couple cardiac muscarinic receptors to a K channel. *Nature* **317,** 536–538
4. Soejima, M., and Noma, A. (1984) Mode of regulation of the ACh-sensitive K channel by the muscarinic receptor in rabbit atrial cells. *Pflügers Arch.* **400,** 424–431
5. Finley, M., Arrabit, C., Fowler, C., Suen, K. F., and Slesinger, P. A. (2004) βL-βM loop in the C-terminal domain of G protein-activated inwardly rectifying K^+ channels is important for $G_{\beta\gamma}$ subunit activation. *J. Physiol.* **555,** 643–657
6. Wickman, K., Nemec, J., Gendler, S. J., and Clapham, D. E. (1998) Abnormal heart rate regulation in GIRK4 knockout mice. *Neuron* **20,** 103–114
7. Signorini, S., Liao, Y. J., Duncan, S. A., Jan, L. Y., and Stoffel, M. (1997) Normal cerebellar development but susceptibility to seizures in mice lacking G protein-coupled, inwardly rectifying K^+ channel GIRK2. *Proc. Natl. Acad. Sci. U.S.A.* **94,** 923–927
8. Slesinger, P. A., Stoffel, M., Jan, Y. N., and Jan, L. Y. (1997) Defective γ-aminobutyric acid type B receptor-activated inwardly rectifying K^+ currents in cerebellar granule cells isolated from weaver and Girk2-null mutant mice. *Proc. Natl. Acad. Sci. U.S.A.* **94,** 12210–12217
9. Blednov, Y. A., Stoffel, M., Chang, S. R., and Harris, R. A. (2001) Potassium channels as targets for ethanol: studies of G protein-coupled inwardly rectifying potassium channel 2 (GIRK2)-null mutant mice. *J. Pharmacol. Exp. Ther.* **298,** 521–530
10. Krapivinsky, G., Gordon, E. A., Wickman, K., Velimirović, B., Krapivinsky, L., and Clapham, D. E. (1995) The G protein-gated atrial K^+ channel IKACh is a heteromultimer of two inwardly rectifying K^+ channel proteins. *Nature* **374,** 135–141
11. Kim, D., Watson, M., and Indyk, V. (1997) ATP-dependent regulation of a G protein-coupled K^+ channel (GIRK1/GIRK4) expressed in oocytes. *Am. J. Physiol.* **272,** H195–H206
12. Logothetis, D. E., Kurachi, Y., Galper, J., Neer, E. J., and Clapham, D. E. (1987) The βγ subunits of GTP-binding proteins activate the muscarinic K^+ channel in heart. *Nature* **325,** 321–326
13. Kobayashi, T., and Ikeda, K. (2006) G protein-activated inwardly rectifying potassium channels as potential therapeutic targets. *Curr. Pharm. Des.* **12,** 4513–4523
14. Kovoor, P., Wickman, K., Maguire, C. T., Pu, W., Gehrmann, J., Berul, C. I., and Clapham, D. E. (2001) Evaluation of the role of $I(K_{ACh})$ in atrial fibrillation using a mouse knockout model. *J. Am. Coll Cardiol.* **37,** 2136–2143
15. Menke, J., Lüthje, L., Kastrup, A., and Larsen, J. (2010) Thromboembolism in atrial fibrillation. *Am. J. Cardiol.* **105,** 502–510
16. Hughes, M., and Lip, G. Y. (2008) Stroke and thromboembolism in atrial fibrillation: a systematic review of stroke risk factors, risk stratification schema, and cost effectiveness data. *Thromb. Haemost.* **99,** 295–304
17. Bettahi, I., Marker, C. L., Roman, M. I., and Wickman, K. (2002) Contribution of the Kir3.1 subunit to the muscarinic-gated atrial potassium channel I_{KACh}. *J. Biol. Chem.* **277,** 48282–48288
18. Rosenhouse-Dantsker, A., Leal-Pinto, E., Logothetis, D. E., and Levitan, I. (2010) Comparative analysis of cholesterol sensitivity of Kir channels: role of the CD loop. *Channels* **4,** 63–66
19. Vivaudou, M., Chan, K. W., Sui, J. L., Jan, L. Y., Reuveny, E., and Logothetis, D. E. (1997) Probing the G protein regulation of GIRK1 and GIRK4, the two subunits of the KACh channel, using functional homomeric mutants. *J. Biol. Chem.* **272,** 31553–31560
20. Lee, A. G. (2003) Lipid-protein interactions in biological membranes: a structural perspective. *Biochim. Biophys. Acta* **1612,** 1–40
21. Marius, P., Zagnoni, M., Sandison, M. E., East, J. M., Morgan, H., and Lee, A. G. (2008) Binding of anionic lipids to at least three nonannular sites on the potassium channel KcsA is required for channel opening. *Biophys. J.* **94,** 1689–1698
22. Sunshine, C., and McNamee, M. G. (1994) Lipid modulation of nicotinic acetylcholine receptor function: the role of membrane lipid composition and fluidity. *Biochim. Biophys. Acta* **1191,** 59–64
23. Jones, O. T., and McNamee, M. G. (1988) Annular and nonannular binding sites for cholesterol associated with the nicotinic acetylcholine receptor. *Biochemistry* **27,** 2364–2374
24. Rankin, S. E., Addona, G. H., Kloczewiak, M. A., Bugge, B., and Miller, K. W. (1997) The cholesterol dependence of activation and fast desensitization of the nicotinic acetylcholine receptor. *Biophys. J.* **73,** 2446–2455
25. Shouffani, A., and Kanner, B. I. (1990) Cholesterol is required for the reconstruction of the sodium- and chloride-coupled, γ-aminobutyric acid transporter from rat brain. *J. Biol. Chem.* **265,** 6002–6008
26. He, C., Yan, X., Zhang, H., Mirshahi, T., Jin, T., Huang, A., and Logothetis, D. E. (2002) Identification of critical residues controlling G protein-gated inwardly rectifying K^+ channel activity through interactions with the βγ subunits of G proteins. *J. Biol. Chem.* **277,** 6088–6096
27. Zhang, H., He, C., Yan, X., Mirshahi, T., and Logothetis, D. E. (1999) Activation of inwardly rectifying K^+ channels by distinct $PtdIns(4,5)P_2$ interactions. *Nat. Cell Biol.* **1,** 183–188
28. Murata, Y., and Okamura, Y. (2007) Depolarization activates the phosphoinositide phosphatase Ci-VSP, as detected in *Xenopus* oocytes coexpressing sensors of PIP_2. *J. Physiol.* **583,** 875–889
29. Christian, A. E., Haynes, M. P., Phillips, M. C., and Rothblat, G. H. (1997) Use of cyclodextrins for manipulating cellular cholesterol content. *J. Lipid Res.* **38,** 2264–2272
30. Kitamura, H., Yokoyama, M., Akita, H., Matsushita, K., Kurachi, Y., and Yamada, M. (2000) Tertiapin potently and selectively blocks muscarinic K^+ channels in rabbit cardiac myocytes. *J. Pharmacol. Exp. Ther.* **293,** 196–205
31. Wang, Z., Yue, L., White, M., Pelletier, G., and Nattel, S. (1998) Differential distribution of inward rectifier potassium channel transcripts in human atrium versus ventricle. *Circulation* **98,** 2422–2428
32. Epshtein, Y., Chopra, A. P., Rosenhouse-Dantsker, A., Kowalsky, G. B., Logothetis, D. E., and Levitan, I. (2009) Identification of a C terminus domain critical for the sensitivity of Kir2.1 to cholesterol. *Proc. Natl. Acad. Sci. U.S.A.* **106,** 8055–8060
33. Romanenko, V. G., Fang, Y., Byfield, F., Travis, A. J., Vandenberg, C. A., Rothblat, G. H., and Levitan, I. (2004) Cholesterol sensitivity and lipid raft targeting of Kir2.1 channels. *Biophys. J.* **87,** 3850–3861
34. Romanenko, V. G., Rothblat, G. H., and Levitan, I. (2002) Modulation of endothelial inward-rectifier K^+ current by optical isomers of cholesterol. *Biophys J.* **83,** 3211–3222
35. Gurdon, J. B., Lane, C. D., Woodland, H. R., and Marbaix, G. (1971) Use of frog eggs and oocytes for the study of messenger RNA and its translation in living cells. *Nature* **233,** 177–182
36. Rishal, I., Porozov, Y., Yakubovich, D., Varon, D., and Dascal, N. (2005) Gβγ-dependent and Gβγ-independent basal activity of G protein-activated K^+ channels. *J. Biol. Chem.* **280,** 16685–16694
37. Huang, C. L., Feng, S., and Hilgemann, D. W. (1998) Direct activation of inward rectifier potassium channels by PIP_2 and its stabilization by Gβγ. *Nature* **391,** 803–806
38. Lopes, C. M., Zhang, H., Rohacs, T., Jin, T., Yang, J., and Logothetis, D. E. (2002) Alterations in conserved Kir channel-PIP_2 interactions underlie channelopathies. *Neuron* **34,** 933–944
39. Rosenhouse-Dantsker, A., Sui, J. L., Zhao, Q., Rusinova R., Rodríguez-Menchaca, A. A., Zhang, Z., and Logothetis, D. E. (2008) A sodium-mediated structural switch that controls the sensitivity of Kir channels to $PtdIns(4,5)P_2$. *Nat. Chem. Biol.* **4,** 624–631
40. Bourne, H. R., Sanders, D. A., and McCormick, F. (1990) The GTPase superfamily: a conserved switch for diverse cell functions. *Nature* **348,** 125–132
41. Bourne, H. R., Sanders, D. A., and McCormick, F. (1991) The GTPase superfamily: conserved structure and molecular mechanism. *Nature* **349,** 117–127
42. Reuveny, E., Slesinger, P. A., Inglese, J., Morales, J. M., Iñiguez-Lluhi, J. A., Lefkowitz, R. J., Bourne, H. R., Jan, Y. N., and Jan, L. Y. (1994) Activation of the cloned muscarinic potassium channel by G protein βγ subunits. *Na-*

ture **370,** 143–146
43. He, C., Zhang, H., Mirshahi, T., and Logothetis, D. E. (1999) Identification of a potassium channel site that interacts with G protein $\beta\gamma$ subunits to mediate agonist-induced signaling. *J. Biol. Chem.* **274,** 12517–12524
44. Carman, C. V., Barak, L. S., Chen, C., Liu-Chen, L. Y., Onorato, J. J., Kennedy, S. P., Caron M. G., and Benovic, J. L. (2000) Mutational analysis of G$\beta\gamma$ and phospholipid interaction with G protein-coupled receptor kinase 2. *J. Biol. Chem.* **275,** 10443–10452
45. Rosenhouse-Dantsker, A., Logothetis, D. E., and Levitan, I. (2011) Cholesterol sensitivity of KIR2.1 is controlled by a belt of residues around the cytosolic pore. *Biophys. J.* **100,** 381–389
46. Pegan, S., Arrabit, C., Zhou, W., Kwiatkowski, W., Collins, A., Slesinger, P. A., and Choe, S. (2005) Cytoplasmic domain structures of Kir2.1 and Kir3.1 show sites for modulating gating and rectification. *Nat. Neurosci.* **8,** 279–287
47. Fang, Y., Mohler, E. R., 3rd, Hsieh, E., Osman, H., Hashemi, S. M., Davies, P. F., Rothblat, G. H., Wilensky, R. L., and Levitan, I. (2006) Hypercholesterolemia suppresses inwardly rectifying K^+ channels in aortic endothelium *in vitro* and *in vivo*. *Circ. Res.* **98,** 1064–1071
48. Dobrev, D., Friedrich, A., Voigt, N., Jost, N., Wettwer, E., Christ, T., Knaut, M., and Ravens, U. (2005) The G protein-gated potassium current I(K,ACh) is constitutively active in patients with chronic atrial fibrillation. *Circulation* **112,** 3697–3706
49. Cha, T. J., Ehrlich, J. R., Chartier, D., Qi, X. Y., Xiao, L., and Nattel, S. (2006) Kir3-based inward rectifier potassium current: potential role in atrial tachycardia remodeling effects on atrial repolarization and arrhythmias. *Circulation* **113,** 1730–1737
50. Ehrlich, J. R., Cha, T. J., Zhang, L., Chartier, D., Villeneuve, L., Hébert, T. E., and Nattel, S. (2004) Characterization of a hyperpolarization-activated time-dependent potassium current in canine cardiomyocytes from pulmonary vein myocardial sleeves and left atrium. *J. Physiol.* **557,** 583–597
51. Fauchier, L., Pierre, B., de Labriolle, A., Grimard, C., Zannad, N., and Babuty, D. (2008) Antiarrhythmic effect of statin therapy and atrial fibrillation a meta-analysis of randomized controlled trials. *J. Am. Coll Cardiol.* **51,** 828–835
52. Adam, O., Neuberger, H. R., Böhm, M., and Laufs, U. (2008) Prevention of atrial fibrillation with 3-hydroxy-3-methylglutaryl coenzyme A reductase inhibitors. *Circulation* **118,** 1285–1293